AIAA-2000-0642

Rayleigh Scattering Diagnostic for Simultaneous Measurements of Dynamic Density and Velocity

Richard G. Seasholtz
NASA Glenn Research Center
Cleveland, OH

J. Panda
Modern Technologies Corp.
Middleburg Hts., OH

38th Aerospace Sciences Meeting & Exhibit
10-13 January 2000 / Reno, NV

Rayleigh Scattering Diagnostic for Simultaneous Measurements of Dynamic Measurement of Density and Velocity

Richard G. Seasholtz*
NASA Lewis Research Center
Cleveland, OH 44135

J. Panda†
Modern Technologies Corporation
Middleburg Hts., OH 44130

Abstract

A flow diagnostic technique based on the molecular Rayleigh scattering of laser light is used to obtain dynamic density and velocity data in turbulent flows. The technique is based on analyzing the Rayleigh scattered light with a Fabry-Perot interferometer and recording information about the interference pattern with a multiple anode photomultiplier tube (PMT). An artificial neural network is used to process the signals from the PMT to recover the velocity time history, which is then used to calculate the velocity power spectrum. The technique is illustrated using simulated data. The results of an experiment to measure the velocity power spectrum in a low speed (100 m/sec) flow are also presented.

Introduction

In this paper we describe a flow diagnostic based on the molecular Rayleigh scattering of laser light. The objective of the work is to develop an unseeded, nonintrusive dynamic measurement technique for the study of turbulent flows in NASA test facilities to provide aerothermodynamic data that are not presently available. These data will be important in studies such as the investigation of growth and decay of turbulent fluctuations. The effort is part of the non-intrusive instrumentation development program supporting supersonic and hypersonic propulsion research at the NASA Glenn Research Center. This work is directed to the measurement of fluctuations in flow velocity, density, and temperature for jet noise studies. One of the main objectives in jet noise research is to identify noise sources in the jet and to determine their contribution to noise generation. In particular, researchers have focused on the correlation of fluctuations in flow parameters with far field noise[1].

A variety of nonintrusive, laser based flow diagnostics (Rayleigh scattering, Laser Doppler Velocimetry (LDV), Particle Imaging Velocimetry (PIV), Laser Induced Fluorescence (LIF)) are routinely being applied for time average and instantaneous planar measurements of velocity, density, temperature, and species concentrations. However, an important class of measurements, high frequency response dynamic measurements of flow parameters, is not addressed by current laser diagnostics. This type of time history data is needed to determine, for example, density and velocity spectra, density-velocity correlations, and two-point correlations. Although LDV can typically achieve data rates of a few tens of kHz, it is difficult to achieve much higher rates without introducing larger amounts of seed material into the flow. In practice, LDV normally provides mean velocity and a measure of turbulence intensity. Furthermore, the measurements are random in time, which makes it difficult to obtain time history data needed for power spectra. In turbulent flows, LDV measurements are beset by a variety of so-called biasing errors, caused by correlations between the measurement rate and flow properties. Planar techniques, such as PIV and planar Rayleigh scattering, provide a large number of simultaneous measurements in a plane, but are generally limited to low sampling rates, determined by the pulse repetition rate of the laser and by the time needed to transfer image data from the camera. New techniques are needed to provide nonintrusive, dynamic measurements that can provide data similar to that provided by hot wire anemometers. Since it is unrealistic to expect (at least at the present time) to make measurements at a large number of locations and at a high sampling rate, it seems prudent to develop a laser diagnostic capable of point measurements at high sampling rates.

Because the Rayleigh scattering technique under study is based on molecular scattering, rather the particle scattering, no seed material need be injected into the flow. One difficulty with LDV and PIV is that they require the flow to be "seeded" with micron seed particles to provide a sufficient concentration of scattering centers. The reliance on seed particles presents a number of

* Senior Research Engineer, Member AIAA
† Senior Research Engineer, Member AIAA

difficulties. It is difficult to inject a uniform cloud of seed in many test facilities, and the seed material must withstand the flow environment. For high temperatures refractory seed materials are necessary. In addition, seed material can contaminate the facility, coating surfaces and windows. Facility engineers are often wary of the introduction of this foreign, often abrasive material, into their equipment. A further limitation of particle scattering methods is that the particles, although small, may not be able to follow large flow accelerations, thus introducing inaccuracy in the prediction of the gas velocity.

These problems associated with particle scattering measurements are eliminated if molecular scattering is used, since the gas molecules that constitute the flow under study are used as the scattering centers. The simplest molecular scattering based diagnostic is Rayleigh scattering. The frequency spectrum of Rayleigh scattering is closely related to the velocity distribution of the scattering gas. The spectrum may be analyzed to determine temperature, density, and velocity. Density is simply proportional to the total scattered light; temperature is related to the width of the Rayleigh spectrum; and one component of velocity is proportional to the shift of the spectra peak from the frequency of the incident light. Because the spectral width is also a function of the molecular weight of the gases in the flow, knowledge of the gas composition is generally required; however, this is not a concern in the proposed work, which is directed toward air flows where the composition is well defined. In any case, velocity measurements, because they are determined from the frequency of the peak of the spectrum, are independent of the gas composition. Rayleigh scattering is particularly suitable for measurement of supersonic and hypersonic velocity where the mean molecular velocity (flow velocity) is larger than the random molecular velocity (temperature).

Because of the relative simplicity of Rayleigh scattering based gas density measurements, they have been more widely used than velocity and temperature measurements. In our work, for example, time and phase averaged density measurements have been made in an underexpanded supersonic free jet in support of jet noise studies[2]. We have also demonstrated simultaneous multiple point density measurements for determining gas density fluctuation spectra, cross-spectra, and cross correlation functions in a low speed heated jet[3].

The more difficult problem of dynamic velocity and temperature measurements was first addressed in a previous paper[4]. That scheme used direct imaging of the Rayleigh scattered light through a Fabry-Perot interferometer. One PMT was used to detect the total Rayleigh scattered light for density measurements (as is done in the present paper). Two additional PMT's were used to determine the velocity and temperature. This method, however, had the disadvantage that it required the detection system, including the sensitive Fabry-Perot interferometer, be located close to the experiment. Also, because only two detectors were used to resolve the Rayleigh scattering spectrum for the velocity and temperature measurement, the scattered light was not efficiently used. In this paper we present an improved version of that system.

One of the new features is that an optical fiber is used to transmit the Rayleigh scattered light from the test region to the Fabry-Perot interferometer (FPI). This will allow the interferometer to be located in a controlled environment where the temperature can be held constant and where acoustic noise and vibration can be minimized. The other new feature is that an 8x8 multiple anode photomultiplier tube is used to detect the interference pattern formed by the FPI. This permits more information to be extracted from the scattered light. Finally, a new PC based data acquisition system is used that can digitize at a rate up 1.2 MHz. In the work described here, we use ten elements of a multiple anode PMT for velocity measurements. One additional separate PMT is used to detect the total Rayleigh scattered light for density determination. Temperature measurements are not addressed in this paper.

The paper first presents some basic background material related to molecular Rayleigh scattering. The lower bounds for measurement of density, temperature, and velocity are given assuming errors result only from Poisson noise generated in the photo detection process. This establishes the best possible measurements that could only be approached by use of an ideal instrument. We then describe the scheme used to measure velocity based on a Fabry-Perot interferometer and a multiple anode PMT. The lower bounds for velocity measurement uncertainties are then calculated for this particular system.

In previous work with time-average measurements, we used non-linear least squares parameter estimation techniques to obtain the flow parameters from the measured interference pattern. Because this is an iterative process, it is rather slow and is not suitable for processing the very large number of individual measurements (~200,000) obtained in this work. Instead, we developed another data processing technique based on artificial neural networks. The network is trained using numerically generated data based on a mathematical model of the optical system. Once trained, the network can rapidly process the large amount of data. We first test the technique using artificial data based on an assumed velocity turbulence intensity and power spectrum.

An experiment is then described that was conducted to evaluate the technique on a low speed flow (up to about 100 m/sec). Preliminary results are given for

velocity time history and for the power spectrum of velocity fluctuations in the flow downstream of a sphere located in the flow.

Theory

Rayleigh scattering

For the purposes of this paper we consider Rayleigh scattering from a low density gas. The spectrum for this situation has a Gaussian profile given by

$$S(f-f_o)df = \frac{2\sqrt{\pi}}{aK}\exp\left\{-\left[\frac{2\pi(f-f_o)-\mathbf{K}\cdot\mathbf{u}}{aK}\right]^2\right\}df \quad (1)$$

where f_o is the laser frequency and $\mathbf{u}$ is the mean gas velocity. The interaction wave vector is $\mathbf{K} = \mathbf{k}_s - \mathbf{k}_o$ (with $\mathbf{k}_o$ and $\mathbf{k}_s$ being the wave vectors of the incident and scattered light), and $a = (2\kappa T/m)^{1/2}$ is the most probable molecular speed (with κ being Boltzmann's constant, m the molecular mass, and T the gas temperature. Note that the spectral peak is shifted by a frequency proportional to the component of the bulk velocity in the K direction. The spectral width is proportional to the square root of the gas temperature. It is convenient to introduce the velocity component $u_K = \mathbf{K}\cdot\mathbf{u}/K$, which represents the measured velocity component.

The assumption of a Gaussian shaped Rayleigh scattering spectrum is only valid if

$$y = \frac{p}{\eta Ka} << 1$$

where p is the gas pressure and η is the shear viscosity. Collective effects of the molecular motions become important for higher density gases ($y \sim 1$) and a more detailed kinetic theory model, such as the Tenti S6 model[5] is required to describe the Rayleigh scattering spectrum. To simplify the analysis presented here, we use the Gaussian spectral model. However the Tenti spectrum does differ somewhat from the Gaussian spectrum for the conditions encountered in this work[4] ($y \cong 0.8$). A more accurate analysis would use the Tenti spectral model.

Lower bounds for ideal measurements

Since Rayleigh scattering is a relatively weak process, the uncertainty in the measurements often is set by the photon statistical noise (shot noise), which determines the lower bound on measurement uncertainty. For example, the variance in the number of photoelectron counts for a Poisson process is equal to the mean number of counts. Thus the lower bound for the relative uncertainty in the measurement of gas density ρ, is equal to the square root of the variance divided by the mean counts. The lower bounds for temperature and velocity uncertainties have also been evaluated for a low-density, one-component gas. The relative uncertainties caused by photon statistics for this case can be written [6,7].

$$\frac{\sigma(\rho)}{\rho} = \left(\frac{1}{N_R}\right)^{1/2}, \quad \frac{\sigma(T)}{T} = \left(\frac{2}{N_R}\right)^{1/2}, \quad \sigma(u_K) = \frac{a}{(2N_R)^{1/2}} \quad (2)$$

These relations provide a lower bound for the measurement uncertainties, which can only be approached if the shot noise is the dominant noise and if an ideal instrument is used. Note that the lower bounds for the uncertainties of density, temperature, and velocity are all inversely proportional to the square root of the number of detected photons.

Lower bounds for practical instrument

Estimates of the measurement uncertainty for the technique described here, where the Rayleigh scattered light is analyzed with a planar mirror Fabry-Perot interferometer, are obtained by numerically calculating the Cramer-Rao lower bound[8]. The variance of the estimate of a parameter α_i (e.g., temperature or velocity) is given by

$$V(\alpha_i) = \left[\Gamma^{-1}\right]_{ii} \quad (3)$$

where no summation over repeated indices is implied. For Poisson statistics, Γ is the Fisher information matrix with elements

$$\Gamma_{ij} = \sum_q \frac{1}{\langle N_{D_q}\rangle}\frac{\partial\langle N_{D_q}\rangle}{\partial\alpha_i}\frac{\partial\langle N_{D_q}\rangle}{\partial\alpha_j} \quad (4)$$

where $\langle N_{D_q}\rangle$ is the expected number of counts from the q^{th} photodetector. The summation is over the number of photodetectors. For example, in previous work[9] using a CCD array detector, the summation would be over the pixels in the image being analyzed. For this work, however, a CCD camera cannot be used because of its slow readout rate (typically on the order of 1 second for scientific grade cameras). To achieve the high data acquisition rate desired for dynamic measurements, we use photomultiplier tubes (PMTs), which combine reasonable quantum efficiency with high gain and low-noise. One PMT is used to measure the total Rayleigh scattered light (i.e., the spectrally integrated light), which gives a measurement of the gas density. A multiple anode PMT is used to detect the Rayleigh scattered light that is transmitted through a planar mirror interferometer. To minimize the demand

on the data acquisition system, we only use a limited number of PMT elements (10 for the work presented here).

Consider an experiment with the following parameters: a laser (532 nm) with output power P_o = 5 W, air at STP, probe volume length L_x = 1 mm, f/4 collecting optics (i.e., solid collection angle Ω = 0.05 sr), and efficiency factor ε = 2 %. The rate of detected photons, given by

$$N_R = \frac{\varepsilon P_o n L_x \lambda \Omega}{hc}\left(\frac{d\sigma}{d\Omega}\right)\sin^2\chi \qquad (5)$$

$$= 20 \text{ million counts / sec}$$

In this equation, n is the gas number density, $d\sigma/d\Omega$ is the differential scattering cross section, χ is the angle between the electric field vector of the (linearly polarized) incident light and the direction of the scattered light, h is Planck's constant, and c is the velocity of light. If we wish to obtain independent measurements at a 1 kHz rate, the total number of detectable photons in each period would be 20,000. Equation 2 gives the lower bound for measurement of density, temperature and velocity for each period:

$$\frac{\sigma(\rho)}{\rho} = 0.7\,\%, \qquad \frac{\sigma(T)}{T} = 1.0\,\%, \qquad \sigma(u_K) = 2.1 \text{ m/sec}$$

This shows that high sampling rate Rayleigh scattering measurements are at least feasible. It must be emphasized, however, that these values represent the best possible measurements given an ideal instrument. In practice, we are limited to instruments, such as the Fabry-Perot interferometer used here, which result in significantly higher uncertainties, as described below.

Optical configuration

In order to perform an uncertainty analysis, we first describe the setup (fig. 1) used for the experimental work. Light from a 5W, 532 nm, single-frequency, Nd:Vanadate CW laser was focused by lens L1 (350 mm focal length) to a 150 μm diameter beam at the probe volume. The laser beam was terminated in light trap LT. Rayleigh scattered light is collected and focused by L2 (two 160 mm focal length lenses) into a 1 mm core diameter, 20 m long optical fiber. Appropriate baffles and stops were used to prevent any stray laser light from entering the fiber. The light exiting the fiber is collimated by lens L3 (145 mm focal length) and split into two paths with an uncoated optical flat (BS1). About 10% of the light is reflected and focused by lens L4 (85 mm focal length) onto PMT 1 (quantum efficiency ~ 20 %). This signal is proportional to gas density. The light transmitted by the beamsplitter is directed through a planar mirror Fabry-Perot interferometer (70 mm dia. mirrors, 90 % reflectivity, 10 GHz free spectral range, finesse ~ 20). The light exiting the interferometer is focused by the fringe forming lens, L6. This lens consists of a pair of lenses (f/2 135 mm focal length and f/1.2 50 mm focal length), that has an effective focal 1960 mm.

The fringe pattern formed at the focal plane of this lens pair is detected with an 8x8 multiple anode PMT (quantum efficiency ~ 5 %). A typical calculated image of the inner fringe of Rayleigh scattered light is shown in figure 2. The image shows light from an extended region corresponding to the image of the exit plane of the optical fiber. Note that a flow in the direction of the K vector, which is in the flow direction (fig. 1), results in a positive frequency shift and increasing fringe diameter, while a flow in the direction opposite the K vector results in a negative frequency shift and decreasing fringe diameter.

Additional optics were included to provide a reference image consisting of light at the unshifted laser frequency. To accomplish this, several components could be placed in the optical path using remotely controlled pneumatic actuators. When placed in the beam, mirror M directed laser light through neutral density filter NDF onto a diffuser that scattered light into the optical fiber. Also, a prism assembly (PA) could be placed in the light path between the Fabry-Perot interferometer and the multiple anode PMT. This served to direct light into a standard video camera. The video signal from this camera was digitized by a frame grabber card in a 486 PC. A computer program analyzed this image and generated signals to control the Fabry-Perot mirror alignment[9].

Uncertainty analysis

We now calculate the Cramer-Rao lower bounds for velocity measurements based on the optical configuration described in the previous section. This allows us to conduct parametric studies to determine the optimum configuration for the Fabry-Perot interferometer and for the light detection system. The expected number of photons detected by the q^{th} PMT element is

$$< N_{Dq} > = \iint A_R S_R(f) I_{FP}(f,\theta) r^2 \, df \, dA \qquad (6)$$

where the integrations are over frequency and the area of the q^{th} element, r is the focal length of the fringe forming lens, A_R is the number of photons that would be detected if the Fabry-Perot interferometer were

removed from the system, and I_{FP} is the Fabry-Perot instrument function given by[10]

$$I_{FP}(\psi) = \left[1 + F\sin^2\left(\frac{\psi}{2}\right)\right]^{-1} \quad (7)$$

where ψ is the phase change (neglecting any phase change on reflection) of the light between successive reflections given by

$$\psi(f,\theta) = \frac{4\pi f \mu d \cos\theta}{c} \quad (8)$$

Here, μ is the refractive index of the medium in the Fabry-Perot cavity, d is the Fabry-Perot mirror spacing, θ_r is the angle between the ray and the optic axis, and $F = 1/(\sin^2(\pi/2N_E)$ where N_E is the effective finesse. In general, the image of a monochromatic extended source located in the object plane consists of a series of unequally spaced concentric rings. In this work, however, the field of view is restricted by the diameter of the optical fiber and includes only the inner fringe as shown in figure 2.

We now calculate the lower bounds for velocity and temperature measurement uncertainties based on the detected light with the ten elements of the multiple anode PMT shown in figure 2. The uncertainties are evaluated as a function of the zero velocity fringe order n_o and the flow velocity.

For a given wavelength λ_o, the order of interference at the center of the fringe pattern is given by $2\mu d = (n + n_o)\lambda_o$, where n and n_o represent the integral and fractional parts of the order, respectively[10]. A bright fringe is located on the optical axis if $n_o = 0$. Off axis, the order of interference at angle θ is given by $2\mu d\cos\theta = (n + n_o - n_k)\lambda_o$, where n_k represents the change in the order of interference between the optical axis and the angular radius θ. (Note that a bright fringe occurs at $n_k = n_o$). For small angles, $n_k = \mu d\theta^2/\lambda_o$. The spectral interval included in the region from the optical axis out to θ is $n_k \cdot FSR$, where the free spectral range $FSR = c/2d$. It follows that the spectral interval between orders n_{k1} and n_{k2} is $(n_{k2} - n_{k1})FSR$. For the purpose of analysis, it is convenient to use the fractional order n_k to describe locations in the Fabry-Perot fringe plane. Because we are working in air, we assume that $\mu = 1$ in the remainder of this analysis.

Note that the actual radius of a fractional order n_x in the focal plane of the fringe forming lens is given by the product of the angle $\theta_x = (\lambda_o n_x/d)^{1/2}$ and the focal length of the fringe forming lens. Also note that the image of the fringe pattern projected back to the fiber exit plane is similarly given by the product of the angle and focal length of the collimating lens.

The lower bound for velocity uncertainty was numerically evaluated as a function of the fringe order n_o and the velocity using equations 1, 3, 4, 6, 7, and 8. For this calculation, three unknown parameters were assumed (i.e., the α_i in eq. 3 were A_R, u_k, and T). The results are shown in figure 3 for the optical system described above for a single measurement using 5 mJ of laser energy (i.e, a measurement made in a 1 msec time interval using a 5 W laser). Note that the minimum uncertainty for velocity measurements depends on the fringe order n_o and velocity. Thus, the fringe order should be set to minimize the velocity uncertainty for the expected velocity. In this example, the minimum uncertainty is about 18 m/sec. As discussed above, an ideal measurement for a 1 ms time would have an uncertainty of about 2 m/sec. Thus, for our FPI based measurement system, the expected velocity uncertainty is about an order-of-magnitude larger than the uncertainty using an ideal instrument.

Experiment

Setup

The optical system described above and shown in figure 1 (with the laser output power equal 5 W) was used to measure the flow in a subsonic free jet (15.9 mm exit diameter). A 3.0 mm diameter sphere was placed at the exit plane of the jet to generate turbulence. The probe volume was 18 mm from the exit plane. The laboratory compressed air supply used for the jet was passed through a three stage filter to remove particles and oil vapor. As shown in figure 1, the jet axis bisected the incident and scattered light directions. With this configuration, the measured velocity component was the jet axial component. Since the flow velocity was in the same direction as the K vector, the frequency shift was positive. Thus the Fabry-Perot interferometer fringe diameter of the Rayleigh scattered light increased as the flow velocity increased. An electronic pressure gauge was used to measure the total pressure in the nozzle plenum. These pressure measurements were used to calculate the flow velocity and temperature using the isentropic flow relations. A high precision electronic thermometer was used to monitor the temperature within the FPI enclosure to correlate interferometer stability with temperature. A PC based data acquisition system was used to record the signals from the PMT's. The load resistors (100 kΩ) for each channel were selected to give a 3 dB frequency cutoff of about 1 kHz, so the velocity uncertainty was expected to be similar to that shown on figure 3. Each channel was digitized at a 20 kHz rate for 25 seconds, resulting in 500,000 samples for each channel. Although the separate PMT for density measurements was included in the setup to give simultaneous velocity

and density measurements, the emphasis was placed on measuring velocity fluctuations since the density fluctuations were expected to be small for the low Mach number flow used in the experiment. Examples of power spectra of density fluctuations measured in a flow with larger density fluctuations are given references 3 and 11.

Data processing

Because of the large number of measurements (> 100,000), previous data processing methods based on weighted nonlinear least squares fitting algorithms are not practical. The least squares algorithms are slow because they are iterative and involve numerical integrations over each detector pixel. A new procedure based on an artificial neural network (ANN) was developed to allow rapid processing of the raw data from the ten channels of the multiple anode PMT.

The first step was to generate a training set for the network. A mathematical model of the optical configuration was used for a range of velocities of 0 to 250 m/sec. In the experimental work, the center position and order of the fringe needed for the model were obtained by analyzing the unshifted reference laser light with a least squares algorithm.

A commercial artificial neural network software package was used to generate and train the network. A feed forward network with one hidden layer of six nodes was used. The input to training set consisted of velocities in the range of 0 to 250 m/sec along with the calculated values of the outputs of nine elements of the multiple anode PMT (the CH 0 signal was not used). No noise was included in the training data. The training was continued until the maximum error was less than 1 %. Data, either simulated or experimental, could be processed with the ANN to recover the velocity time record from the PMT signals. The power spectrum was then calculated using the Welch method of modified periodograms.

Welch method of modified periodograms

We used the Welch method of modified periodograms[12] to calculate an estimate of the power spectrum of the velocity fluctuations. In this procedure, a long data record sampled at rate f_s for time T (total samples = $N = Tf_s$) is subdivided into a number K of smaller records (which may be overlapping), each of length L samples. The modified periodograms of each sub-record are calculated using a data window; these individual periodograms are then averaged to obtain the estimate of the power spectrum. The frequency resolution of the resulting spectrum is thus f_s/L. By overlapping the segments by one half of their length, a near maximum reduction in the variance in the spectral estimate is achieved; the variance in the estimated spectrum is reduced by a factor of 11/9K compared to the variance of a single spectral estimate.

Results

Numerical simulation results

The data processing scheme was evaluated using simulated data for a turbulent flow. A simulated velocity time record for turbulent flow was first generated by filtering Gaussian white noise to obtain a time record with the desired power spectrum. The data were then scaled to arrive at the desired mean velocity and turbulence intensity. The model represented by equation 6 was then used to generate the outputs of nine pixels of the multiple anode PMT. Photon statistical noise was accounted for by treating the PMT outputs as a random process with Poisson statistics . Finally the signal was passed through a digital RC low pass filter to simulate the expected frequency rolloff in the experimental data. These simulated signals were then processed by the ANN to recover the velocity record. Finally, an estimate of the power spectrum of the velocity fluctuations was calculated using the Welch method described above.

An example of this process is shown in figure 4. The flow being simulated has a mean velocity of 100 m/sec and a turbulence intensity of 20 %. The velocity power spectrum was assumed to have the shape shown in figure 4a. The sampling rate was 20 kHz and the total number of samples calculated was 256K (262,144), corresponding to a data acquisition time of 13 seconds. The power spectrum of the velocity fluctuations is shown in figure 4b. This was calculated using the Welch method described above with individual record lengths of 2048 samples. A short sample of the outputs of the PMT pixels is shown in figure 4c. Only three (channels 1, 2 & 3) of the nine signals are shown to avoid clutter. These signals were then processed with the ANN. The probability distribution function (PDF) of the velocity record output by the ANN is shown in figure 4d. Note that the standard deviation (31.5 m/sec) is somewhat larger than the standard deviation of the actual velocity fluctuations (20 m/sec). The standard deviation should be the root-sum-square of the turbulence fluctuations and the photon statistical noise, which would be about 28 m/sec. The larger standard deviation may be a result of additional noise created by the ANN processing. Note that the PDF is not symmetric. An estimate of the power spectrum of the velocity fluctuations was then calculated and is shown in figure 4e. Within the bandwidth of the velocity fluctuations, the spectrum is approximately three times the level of the Poisson statistical noise. Lower levels of turbulence intensity would result in less difference between the velocity

fluctuation spectrum and the noise and would eventually set a lower limit on ability to measure the power spectrum of the velocity fluctuations.

Experimental results

An example of data obtained with the optical setup described above is shown in figure 5. The flow velocity calculated from the total pressure and total temperature was 119 m/sec. The sampling rate was 20 kHz and a total of 500,000 samples were obtained for each of ten channels of the multiple anode PMT and for the single channel PMT used for density. Nine of the multiple anode PMT channels were used to obtain dynamic velocity. The signals from each of the nine channels were first scaled by the mean values obtained from the simulation discussed above. This served to compensate for any differences in gain in the nine channels and fixed the mean velocity at 119 m/sec. The data from each channel was also filtered with a digital RC low pass filter with a cutoff frequency of 5 kHz. The data were processed with the ANN trained with the simulated data described in the above section. The velocity probability distribution function is shown in figure 5a (mean of 120 m/sec and a standard deviation of 36 m/sec). In this experiment, turbulence was not independently measured, so it is not possible to separate the effect of flow turbulence from that of shot noise on the standard deviation. The power spectrum of the velocity fluctuations calculated using the Welch method and is shown in figure 5b. The density fluctuation spectrum is shown in figure 5c. The relative standard deviation of the data for the density measurement was 10 %. Since the density fluctuations for this low speed flow should be very small, the fluctuations in the density data were expected to be only caused by the photon statistical noise. The extraneous peaks in the high frequency regimes of the velocity and density spectra are thought to be a result of electrical interference.

Concluding remarks

A new technique for obtaining dynamic velocity measurements using molecular Rayleigh scattering was demonstrated. The velocity was determined by analyzing the scattered light with a Fabry-Perot interferometer. The method was illustrated using simulated data for a turbulent flow with a given velocity power spectrum. Some preliminary experimental data were also presented. This work served to point out several things that must be done in order to successfully apply the technique in test facilities.

The amount of Rayleigh scattered light collected and analyzed must be sufficiently intense to allow the power spectrum of the velocity fluctuations in the frequency range of interest to be greater than the spectrum of the photon statistical noise. For the system discussed in this paper, we showed that a turbulence intensity of 20 % with a 1 kHz bandwidth gave adequate results. For turbulence intensities less than about 10 % or for significantly larger bandwidths, a larger scattered light level would be necessary. This could be achieved in several ways.

First, the laser power could be increased. However, to significantly increase the power above the 5 W used here would be expensive. Second, the quantum efficiency of the multiple anode PMT was only about 5 %. Individual PMT's could be used, which would allow quantum efficiencies up to 20 %. The amount of light collected from the probe volume could be increased by using faster optics, but there are limitations related to the optical fiber numerical aperture and to the etendue of the Fabry-Perot interferometer. Another way to increase the Rayleigh signals would be to use a multiple pass arrangement to pass the laser beam through the probe volume. With one or more of these improvements, this technique should be capable of measuring the power spectrum of velocity fluctuations in turbulent flows of interest for jet noise studies.

Acknowledgments

We would like to acknowledge the efforts of Mr. W. Trevor John, Mr. Bertram Floyd, and Ms. Kristie Elam who were responsible for setting up and aligning the optical system and who assisted in taking the data.

References

[1] Schaffar, M., "Direct measurements of the correlation between axial in-jet velocity fluctuations and far-field noise near the axis of a cold jet", *J. Sound and Vibration*, **64**, pp. 73-83, 1979.

[2] Panda, J., and Seasholtz, R.G., "Measurements of shock structure and shock-vortex interaction in underexpanded jets using Rayleigh scattering", *Phys. Fluids*, **11**, pp. 3761-3777, 1999.

[3] Seasholtz, R., and Panda, J., "Multiple point dynamic gas density measurements using molecular Rayleigh scattering", *18th International Congress on Instrumentation in Aerospace Simulation Facilities Conference*, Toulouse, France, June 14-17, 1999. [also NASA TM-1999—209295].

[4] Seasholtz, R.G., and J. Panda, "Rayleigh scattering diagnostic for dynamic measurement of velocity and temperature", *AIAA 37th Aerospace Sciences Meeting*, Reno, NV, AIAA-99-0641, 1999.

[5] Tenti, G., Boley, C.D. and Desai, R.C., "On the kinetic model description of Rayleigh Brillouin scattering from molecular gases", *Can. J. Phys.* **52**, pp. 285-290, 1974.

[6] Seasholtz, R.G., "High-speed anemometry based on spectrally resolved Rayleigh scattering", *Fourth International Conference on Laser Anemometry*, Cleveland, Ohio, 1991 [also NASA TM-104522].

[7] Seasholtz R.G. and Lock, J.A., "Gas temperature and density measurements based on spectrally resolved Rayleigh-Brillouin scattering", *NASA Langley Measurement Technology Conference*, Hampton, VA, 1992.

[8] Whalen, A.D., *Detection of Signals in Noise*, Academic Press, New York, pp. 324-231, 1971.

[9] Seasholtz, R.G., and Greer, L.C., "Rayleigh scattering diagnostic for measurement of temperature and velocity in harsh environments", *AIAA 36th Aerospace Sciences Meeting*, AIAA-98-0206, Reno, NV, Jan12-15, 1998.

[10] Vaughan, J.M., *The Fabry Perot Interferometer, History, Theory, Practice and Applications*, Adam Hilger, Bristol, pp. 89-112, 1989.

[11] J. Panda, and Seasholtz, R.G., "Density fluctuation measurements in supersonic fully expanded jets using Rayleigh scattering", 5th *AIAA/CEAS Aeroacoustics Conference*, Seattle, WA, AIAA-99-1870, 1999.

[12] Welch, P.D., "The use of fast Fourier transform for the estimation of power spectra: A method based on time averaging over short, modified periodograms", *IEEE Trans. on Audio and Electroacoustics*, **AU-15**, pp. 70-73, 1967.

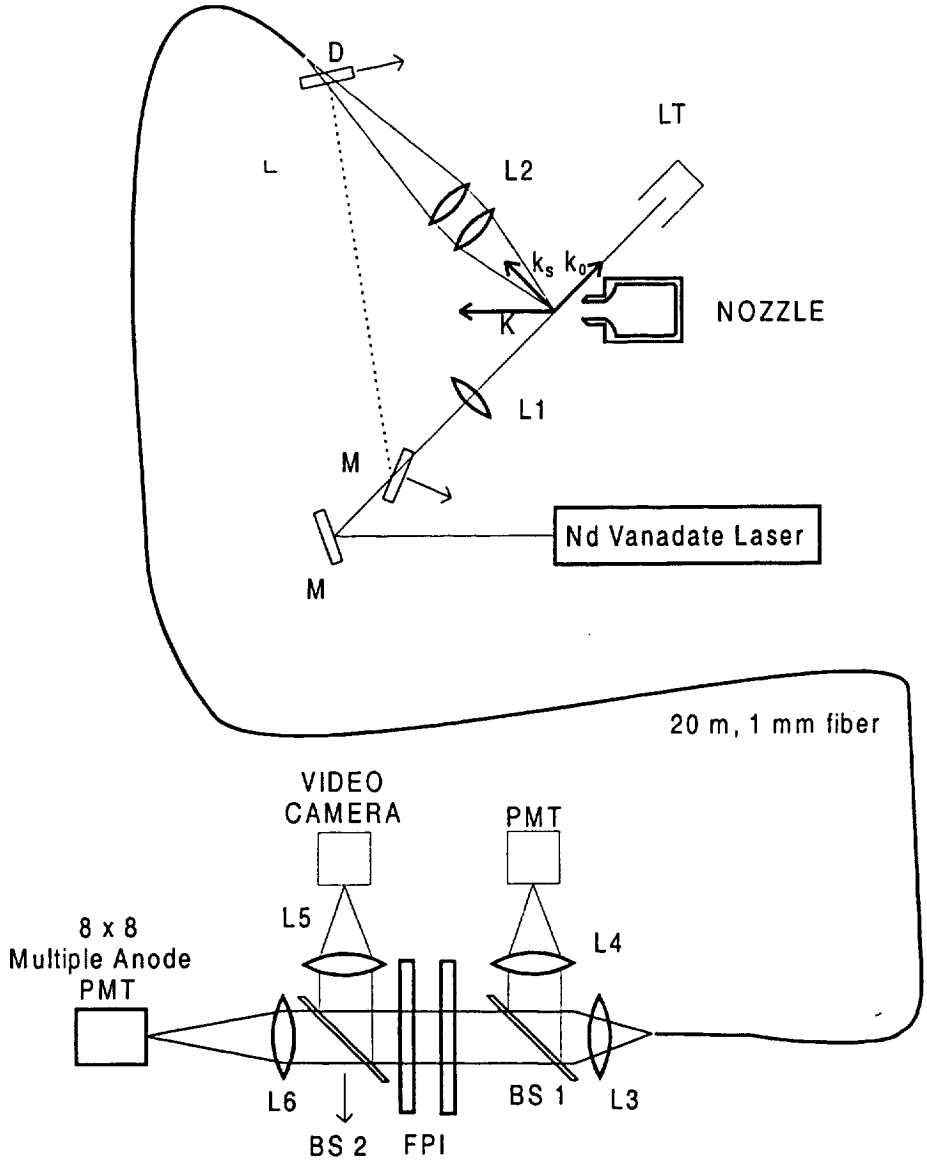

Fig. 1 – Layout of Rayleigh scattering experiment to obtain dynamic density and velocity measurements in turbulent flow; arrows denote components that are mounted on remotely controlled actuators.

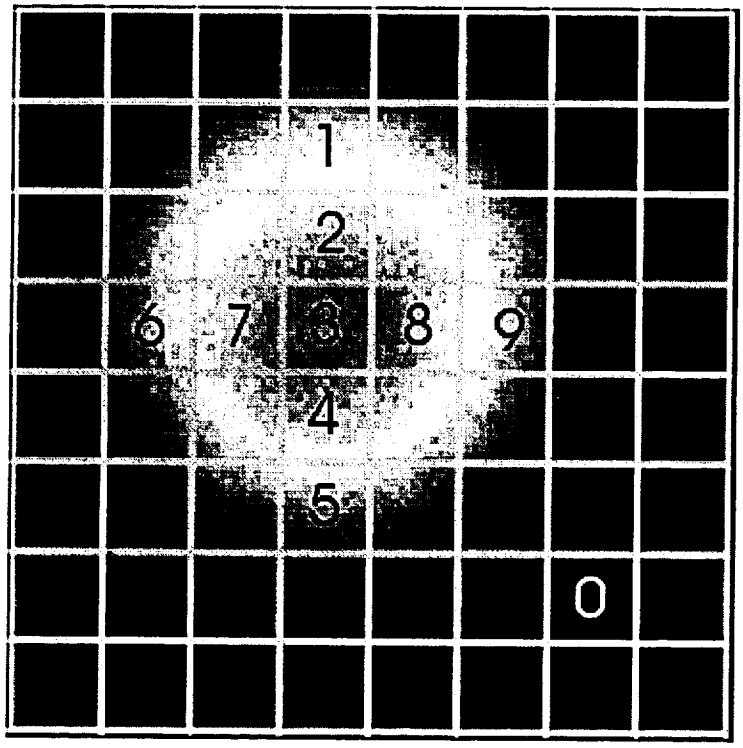

Fig. 2 – Fabry-Perot interferometer fringe pattern superimposed on 8 x 8 multiple anode PMT.

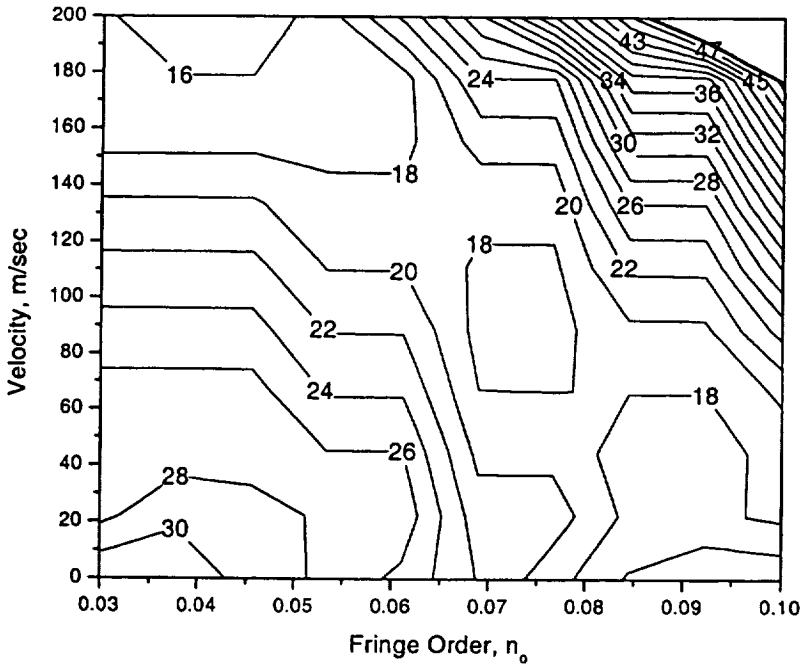

Fig. 3 Predicted uncertainty in velocity (m/sec) as a function of Fabry-Perot interferometer fringe order and velocity.

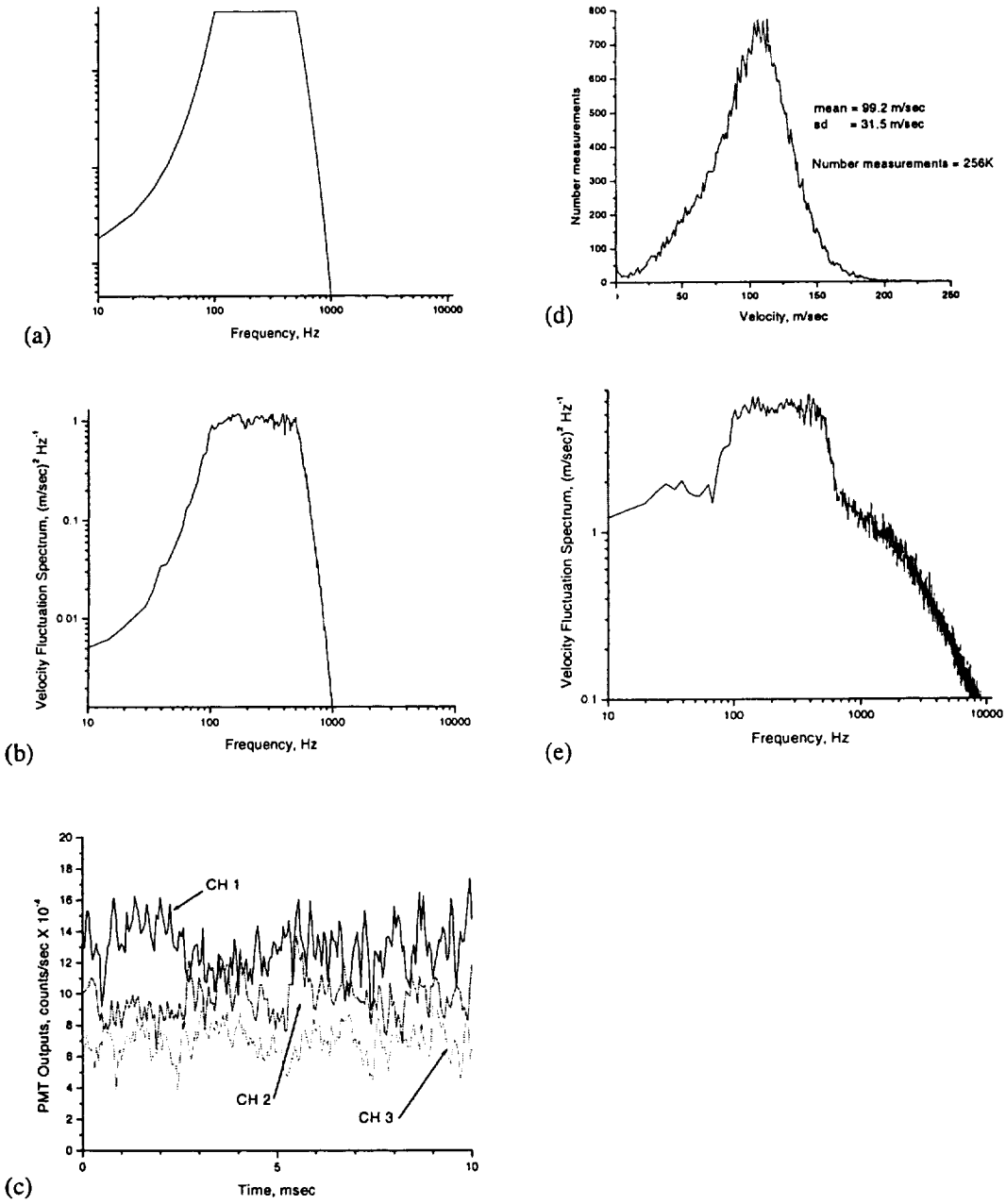

Fig. 4 – Simulation of processing of turbulent velocity signal (mean velocity = 100 m/sec, turbulence intensity = 20 %) with artificial neural network (ANN); (a) power spectrum of model spectrum, (b) power spectrum of simulated velocity, (c) output of three channel of multiple anode PMT, (d) probability distribution function of velocity obtained from ANN, (e) power spectrum of velocity fluctuations obtained from ANN.

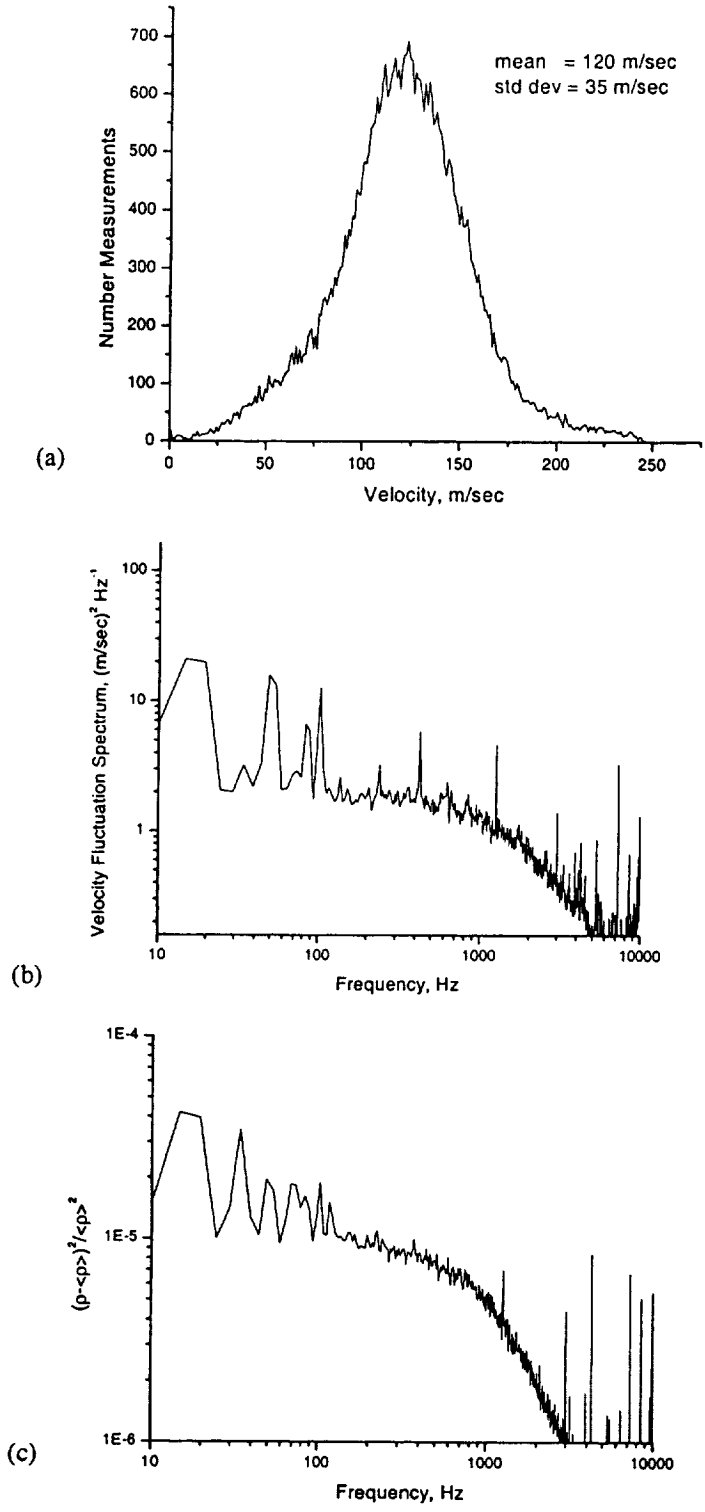

Fig. 5 – Results of experiment to measure velocity and density power spectrum using molecular Rayleigh scattering data processed with artificial neural network (ANN); sampling rate was 20 kHz and bandwidth was limited to 1 kHz, number samples was 256K (a) probability distribution function of velocity obtained from ANN, (b) velocity power spectrum calculated using Welch method of modified periodograms, (c) density fluctuation spectrum.